Compressor Stage Design for Turbojet Engine using Ansys Fluent

B. Bunt, B. Lee, E. Taglia, P. Sklavounos

The Cooper Union for the Advancement of Science & Art

Abstract: This study focuses on the design and optimization of a compressor stage for a new type of gas turbofan engine, aiming to minimize the power required for operation, while satisfying the given performance requirements. A computational fluid dynamics (CFD) approach using ANSYS Fluent is employed to determine the optimal geometry of the compressor rotors and rotor speed. The compressor stage is designed to provide a minimum pressure ratio of 20:1 at maximum design altitude (37,000 ft) and to work efficiently at sea level under standard temperature and pressure (STP) conditions. The outer diameter of the compressor, including all necessary parts, is constrained at 6 ft, and the maximum operating speed of any stage should be less than 50,000 rpm.

Design Statement: A client has commissioned our team to design a compressor stage for a new type of gas turbofan engine that will provide a minimum pressure ratio of 20:1 at a maximum design altitude of 37,000 feet. The compressor will also utilize an optimal geometry and rotor operating speed that confirm with the design constraints for sizing and operating speeds.

Design Benefit: The compressor will minimize power consumption while providing at least the required pressure ratio at both of the specified altitudes.

Design Constraints & Assumptions:

- The compressor shall provide a minimum pressure ratio of 20:1 at maximum design altitude. The compressor can work as a single or multistage unit.
- The engine is being designed to work at a maximum altitude of 37,000'.
- The outer diameter of the compressor should be between 4' and 6'. This includes all of the parts required by your design.
- The maximum operating speed of any stage should be less than 50,000 rpm.
- The engine is tested on a test stand and the entrance condition is operated at subsonic speeds.
- The air entering the engine may be assumed to be at standard conditions for the specific altitude being analyzed.
- The exit condition for the compressor stage is to be an exhaust tube matching the exit diameter of the final stage of your compressor.

I. Materials

<u>Fluids</u>

Air was used as fluid flowing through the turbine engine. At sea level, the given values for its properties from Ansys Fluent's material database were used. At 37,000 ft above sea level, the following values were used (Table 1).

Table 1: Air Properties

Altitude	Air Density (lbm/ft^3)	Air Viscosity (lb/ft s)	Specific Heat (Btu/lbm R)	Thermal Conductivity (Btu/h ft R)
Sea Level (STP)	0.076	1.20e-05	0.240	0.014
37000 ft	0.001756	3.74e-07	0.240	0.00974

<u>Solids</u>

The materials used for the components of the compression section of the turbo engine must withstand high pressures, temperatures, and mechanical stresses. This is why a glass-fiber– shell/ graphite- core was chosen as it is an advanced composite that achieves weight reduction, temperature capability, and durability. [1]

Table 2: Physical Properties of Solid Materials [2]

Property	**Carbon Fiber/Graphite Composite**	**Glass Fiber Composite**
Tensile Strength (ksi)	450	47.5
Compressive Strength (ksi)	180	34
Young's Modulus (Msi)	28	3.75
Flexural Strength (ksi)	285	40
Density (lb/in^3)	0.061	0.0745
Thermal Conductivity (Btu/hr· ft· °F)	5.5	75
Coefficient of Thermal Expansion (1/°F)	0.000002	0.000004

II. Rotor & Stator Design

Figure 1: Rotor design (NACA M8 airfoil)

The geometry of the rotor and stator that was utilized is the NACA M8 airfoil, as shown in the figure above. At ground level the airfoil should maximize static pressure under the wing but produce high lift force and low drag force when in flight. This airfoil was chosen due to its high ratio of lift coefficient to drag coefficient, which is optimal for aerodynamic efficiency [1]. The optimal angle of attack for this angle is 6 degrees, which was implemented as the perpendicular angle of attack of incoming air into the turbofan.

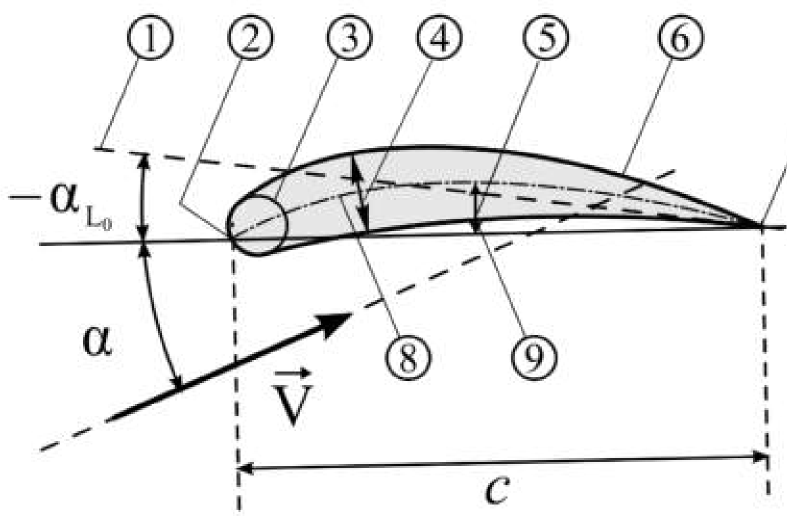

Figure 2: Profile geometry of rotor/stator airfoil [1]

Profile geometry: 1: Zero-lift line; 2: Leading edge; 3: Nose circle; 4: Max. thickness; 5: Camber; 6: Upper surface; 7: Trailing edge; 8: Camber mean-line; 9: Lower surface, c: Chord Length, α: Velocity Angle of Attack, α_{L_0}: Zero Lift Angle

All dimensions are in inches.

III. Hand Calculations

a. Entrance and exit temperatures of air

At Sea Level:

$$T_2 = T_1 \cdot \left(\frac{P_2}{P_1}\right)^{\frac{\Gamma-1}{\Gamma}}$$

Where

$$T_1 = 80°F,\ P_1:P_2 = 1:20$$

And

$$P_1 = 1\,atm,\ P_2 = 20\,atm$$

$$\Gamma = \frac{C_p}{C_v} = \frac{1}{0.718} = 1.4 \text{ at STP}$$

$$T_2 =\cdot \left(\frac{20\,atm}{1\,atm}\right)^{\frac{1.4-1}{1.4}}$$

$$T_2 = 679.17\,F$$

At 37,000 ft:

$$T_{altitude} = T_{sea\ level} + (Lapse\ Rate \cdot Altitude)$$

Tropopause sublayer that has a temperature that decreases linearly with altitude:

Lapse rate: -3.57°F per 1,000 ft

$$T_{37{,}000\,ft} = 80°F + \frac{-3.57 * 37000}{1000} = -70°F$$

$$\boldsymbol{\Gamma = \frac{C_p}{C_v} = 1.4}$$

$$\boldsymbol{T_2 = 213K \cdot \left(\frac{20\,atm}{1\,atm}\right)^{\frac{1.4-1}{1.4}} = 501.3K = 442.67F}$$

b. Power Approximation

Assuming inviscid flow and isentropic compression through the compressor stage, the following method can be used to find the power efficiency:

$$W_{actual} = \dot{m}c_p\,(T_{03} - T_{02})$$

$$\boldsymbol{W_{actual} = 2\frac{lb}{s} * 0.\frac{24BTU}{lbm * R}(1075 - 901) = 84\,kg\frac{m^2}{s^2}}$$

$$W_{adiabatic} = c_p T_{02}\left[\left(\frac{P_{03}}{P_{02}}\right)^{\frac{\gamma-1}{\gamma}} - 1\right]$$

$$W_{adiabatic} = 0.24 * 442[(20)^{\frac{0.4}{1.4}} - 1] = 143\,kg\frac{m^2}{s^2}$$

$$W_{actual} = W_{adiabatic} \cdot \eta_c$$

$$\eta_c = \frac{84}{143} = 0.58$$

$$\eta_t = \frac{W_{adiabatic}}{W_{actual}} = 1.7$$

$$\eta = \frac{T_{04} - T_{02}}{c_p T_{03} - c_p T_{02}} \cdot \frac{1}{PR^{\frac{\gamma-1}{\gamma}}} \cdot \frac{1}{\eta_c \eta_t}$$

$$\eta = 0.82$$

η is the operating efficiency

T_{02} is the compressor inlet temperature

$T_{03}$is the compressor outlet temperature (inlet of combustor)

T_{04} is the turbine exhaust temperature

c_p is the specific heat at constant pressure for the gas mixture in the engine
(This is typically assumed to be around $1000 \frac{J}{kgK}$ for air at high temperatures)

γ is the ratio of specific heats (typically around 1.4 for air)

PR is the pressure ratio

η_c is the compressor efficiency

η_t is the turbine efficiency

Altitude	Power Approximation [kW]	Compressor Efficiency [%]
STP	2.94	82.0
37000	84.17	84.1

IV. Entire Design Assembly

Figure 3: View of Stator /Rotor Design Assembly (inlet at left)

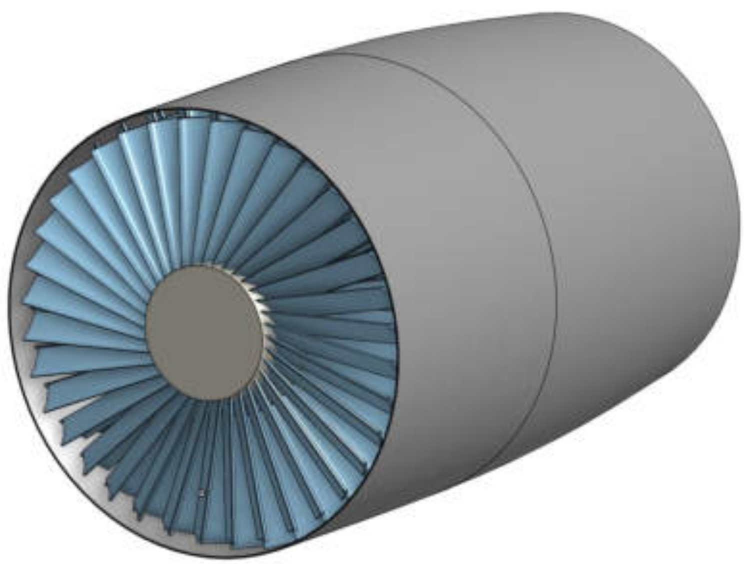

Figure 4: Compressor assembly, with outer shell for further stages (combustion, turbine, exhaust, etc) added behind compressor stages

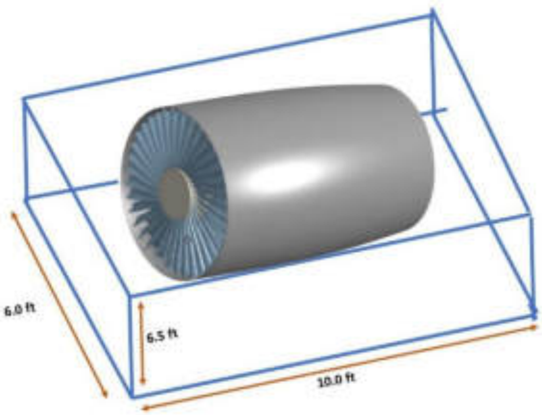

Figure 5: Dimensions of overall device, with height and width being the maximum diameter

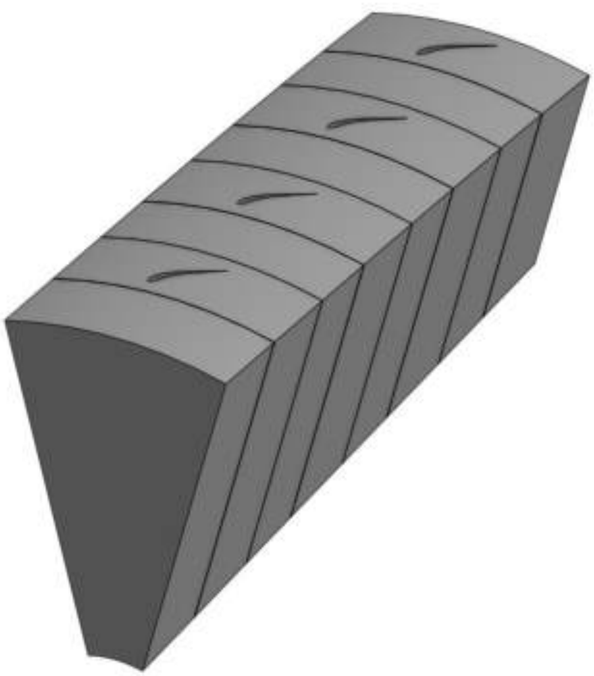

Figure 6 View of portion of compressor for meshing & simulation, with 4 stages of rotor stator pairs (factor of 360 degrees)

V. Scaled Sketches

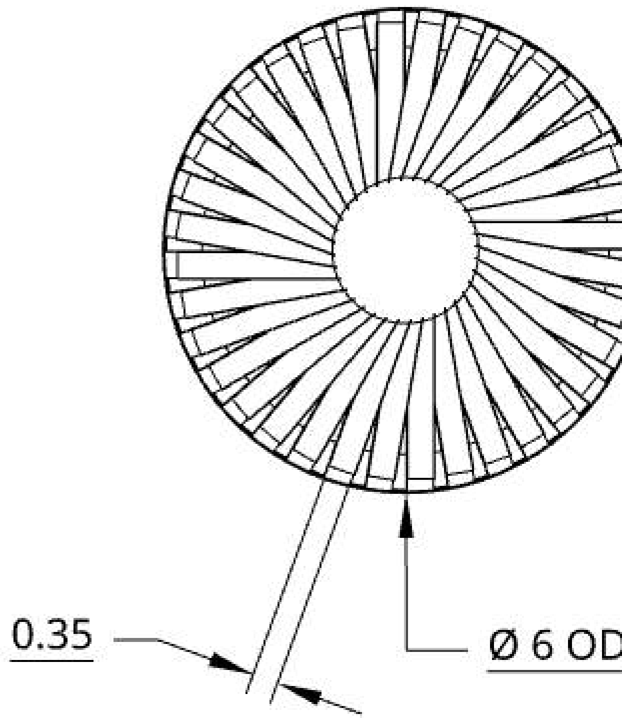

Figure 7: Dimensioned sketch of the front of compressor, looking inward towards rear (units of feet with 2 d.p)

The shell of the compressor has a thickness of 3 inches (0.25 ft).

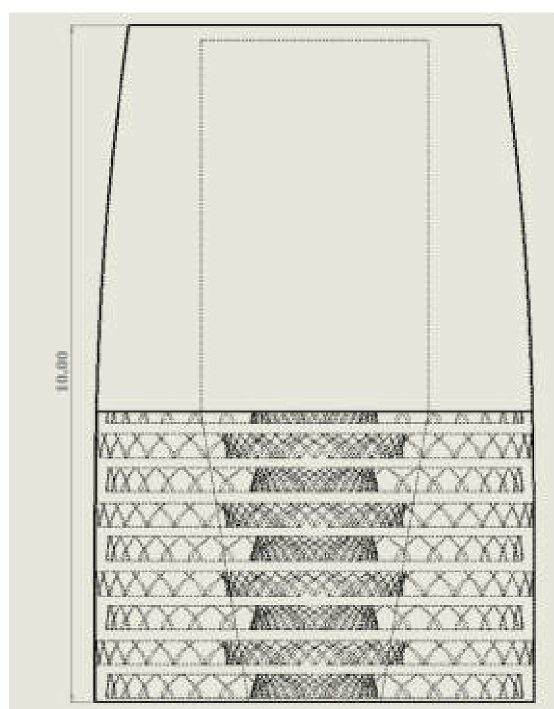

Figure 8: Dimensioned Sketch of Compressor Top View with Hidden Lines Visible

Figure 9: Zoomed in image of the Rotor-Stator combinations of the Figure above

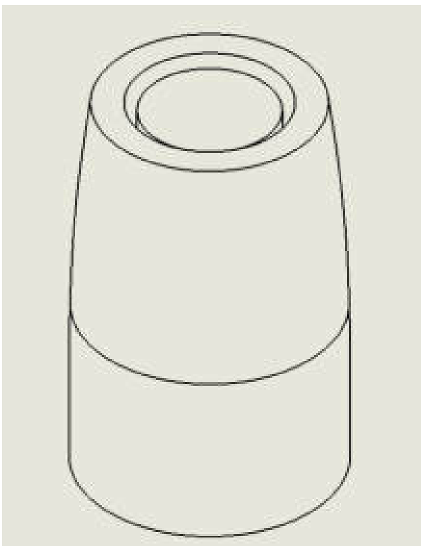

Figure 10 1011: Alternate view of Comopressor

Table 3: Dry weight of Compressor parts

Part	Dry Weight (lb)
Stators & Rotors	280
Hub	3154
Shell	373
Total	**3806**

This order of magnitude is within the range of aircrafts found from different manufacture brochures like the Airbus A320, with the total weight of compressors span from 252lb all the way to 6100lb as seen below. Individual weight for the manufacturers' components was not readily available information.

Table 4: Compilation of Aircrafts, their compression ratio and the total compressor weight[6a-6h]

Aircraft Model	Compression Ratio	Number of Compressor Stages	Compressor Weight
Boeing 737-800	30:1	13	1,560 lb (707 kg)
Airbus A320	30:1	10	1,764 lb (800 kg)
Boeing 747-8	30:1	18	6,056 lb (2,748 kg)
Airbus A380	40:1	16	6,173 lb (2,800kg)
Bombardier CRJ-700	16:1	7	327 lb (148 kg)
Embraer E170	17:1	7	462lb (210 kg)
Gulfstream G650	16.9:1	14	1,636 lb (742 kg)
Cessna Citation X+	8.5:1	2	252 lb (114 kg)
Lockheed Martin F-22 Raptor	N/A	2	1,042 lb (472 kg)
Eurofighter Typhoon	N/A	2	2,314lb (1,050 kg)

VI. Meshing

HyperMesh was used for the design meshing to maximize mesh editing and customization, but to also use less computational resources as Ansys Meshing seemed to be bottlenecking due to the complex geometry and required resolution. An average element size of 0.006 inches was used, with more resolution around areas of interest, such as the stators and rotors.

Figure 11: Quadrilateral Mesh of Exterior Rotor Fluid

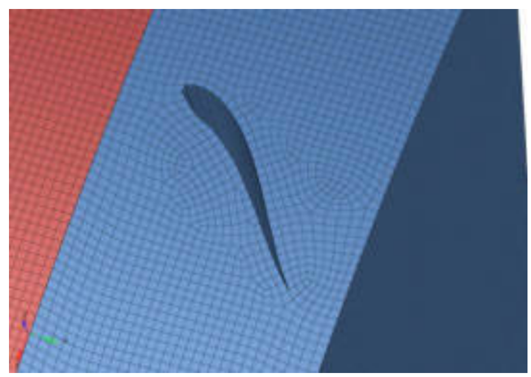

Figure 122: View of Resolution at Stator and Rotor on the Fluid Bodies ensuring 3 cells from walls

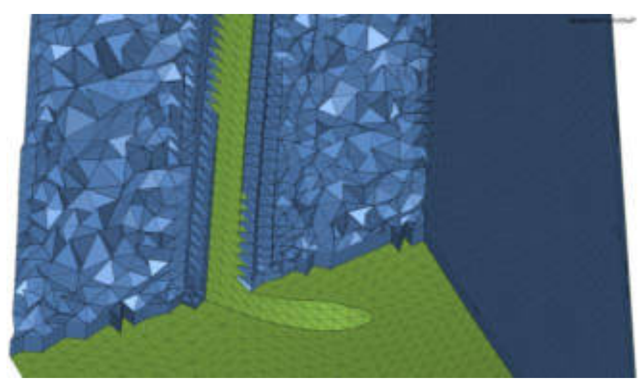

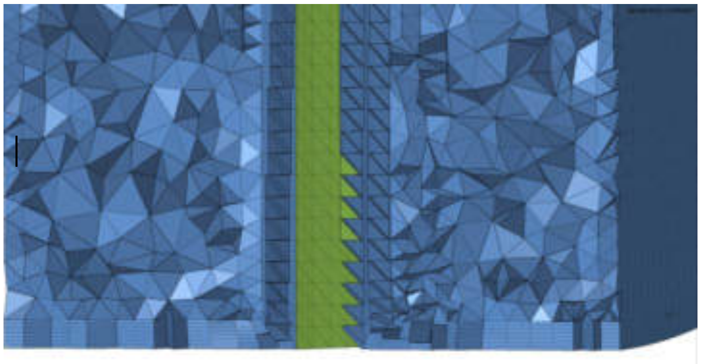

To simplify meshing and the CFD analysis of the model, the model was split into 30ths. A CFD tetramesh was used for the fluid of the stator and rotor with an intersection in between for the mixing plate. Multiple boundary layers around the walls were used. To minimize the overall size of the model, prisms and an inflation factor of 1.2 were used on fluid elements. This allowed for larger element sizes in areas of the geometry where high resolution was not critical. Similar wedge-shaped geometry was replicated for all stages to automate the process. This allowed for periodicity to be used while meshing and running simulations. This way, only one pair for each stage needed to be considered in Fluent. To create a periodic mesh, it is important to use the Hypermesh periodic mesh feature in Mesh>Create>2D Elements>Periodic mesh. By projecting the mesh of the rotor outlet to the interface, and then the interface to the stator inlet, it ensures that the mesh interface can be created, and that data can flow correctly through the model without disjointed cells.

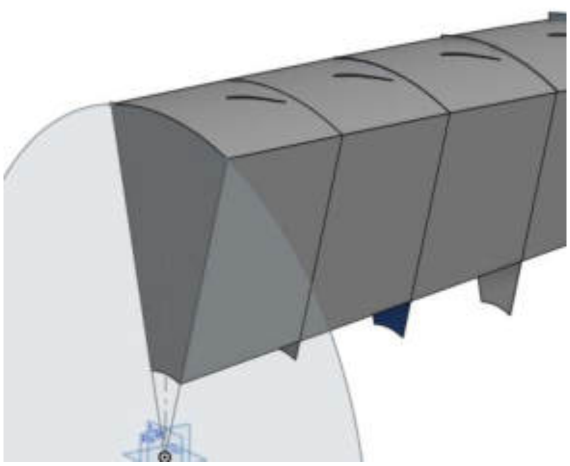

Figure 133: Interfaces between each stage, emphasized by elongating for visibility (fluid body 1/12th slice)

VII. Simulation Results

A sliding mesh model was used to simulate the compressor. This model consisted of dividing the domain into rotating and non-rotating zones. The interfaces are surfaces of revolution about the axis of rotation and are rotationally periodic. The meshes do not deform throughout simulation, and rather stay rigid. The motion of any point in the domain can be given by the time rate of change of the position vector ($\dot{R}$). This is also known as the grid speed. This model was chosen due to its accurate description of flow fields for situations where unsteady interactions occur. It is able to handle multiple rotating domains, each with their own unique rotational axes. The non-conformal mesh interface capability is ~~also~~ useful as it enables an easy toggle between MRF and sliding mesh.

The realizable k-epsilon turbulence model was used with appropriate boundary conditions. More information on the simulation setup is provided in Appendix c.
The following compression ratios were obtained, with their respective operating speeds for each of the 0.5 second intervals of running the simulations to gradually increase the speed.

Operating Conditions

Compression ratio	Operating speed(rpm) @ 1st 0.5s	Operating speed(rpm) @2nd 0.5s	Operating speed(rpm) @3rd 0.5s	Power (kW)
At least 20:1	500	1500	2500	39.4
76:1	20,000	20,000	20,000	314.9

The power usage at each altitude was calculated using the maximum angular velocity. The power usage at operating altitude is comparable to other small jet aircraft.

a. Compressor Case 1 (Atmospheric Conditions at STP)

Table 5: Area Weighted Average Static Temperature at STP

Area-Weighted Average Static Temperature.	Temp [°F]
Rotor Inlet	81.1
Rotor Outlet	80.7
Stator Inlet	80.8
Stator Outlet	80.9

i. Temperature contours

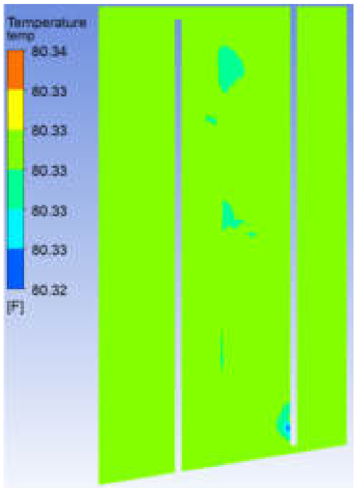

Figure 14: Temperature contour at STP across stage 1

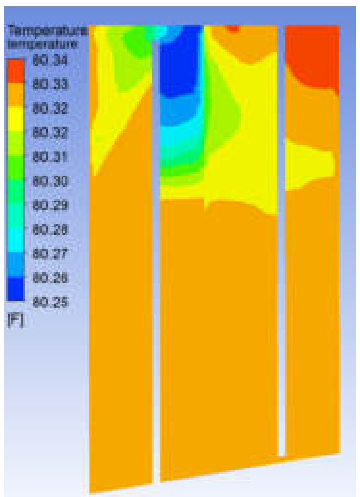

Figure 1514: Temperature contour at STP across stage 2

ii. Pressure Contours

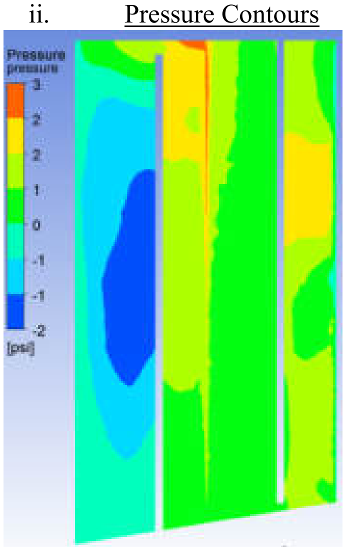

Figure 1615: Pressure Contour at STP across stage 1

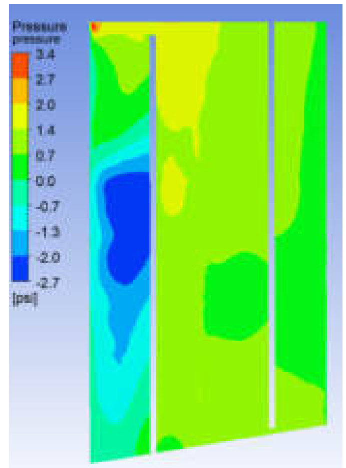

Figure 17 16: Pressure Contour at STP across stage 2

iii. Compression ratios

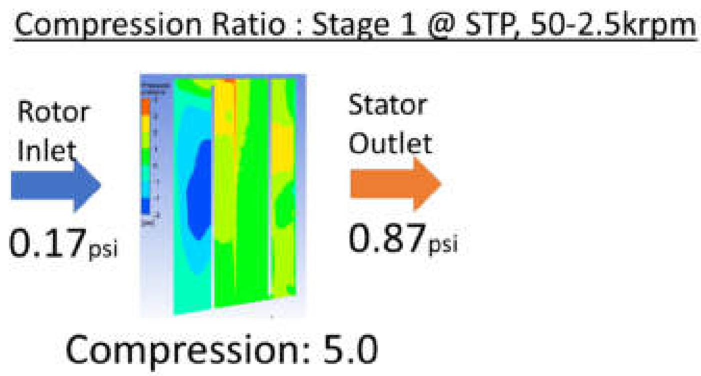

Figure 18: Compression ratio for Stage 1, with variable speed in warming up engine.

Figure 19: Compresion ratio for Stage 2, with variable speed in warming up engine

b. Compressor Case 2 (Flying Conditions at 37000ft)

i. Temperature Contour Plots

Area-Weighted Average Static Temperature	Temp [°F]
Rotor Inlet	-66

Rotor Outlet	-21
Stator Inlet	-13
Stator Outlet	26

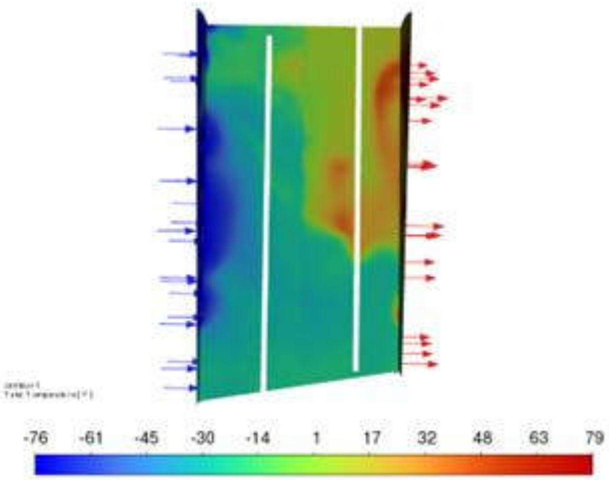

Figure 20: Temperature Contour Across Stage 1

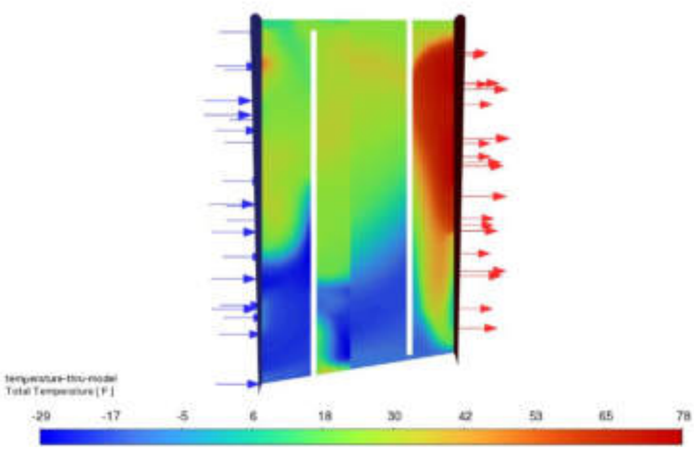

Figure 21: Temperature Contour Across Stage 2

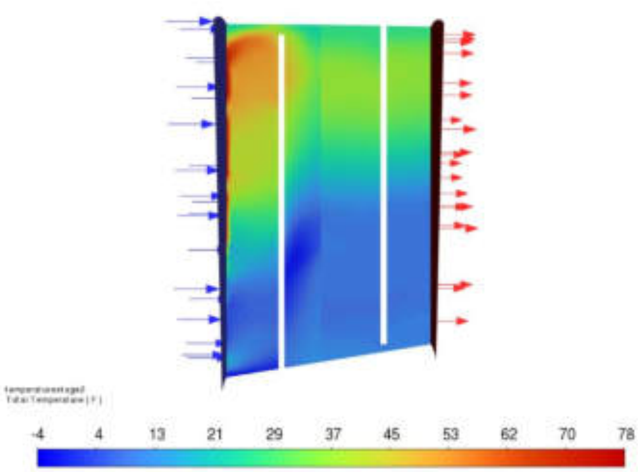

Figure 2217: Temperature Contour Across Stage 3

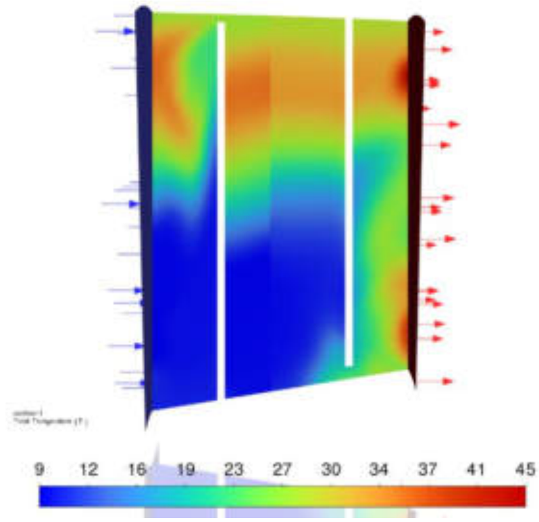

Figure 23: Temperature Contour Across Stage 4

ii. <u>Pressure contour plots</u>

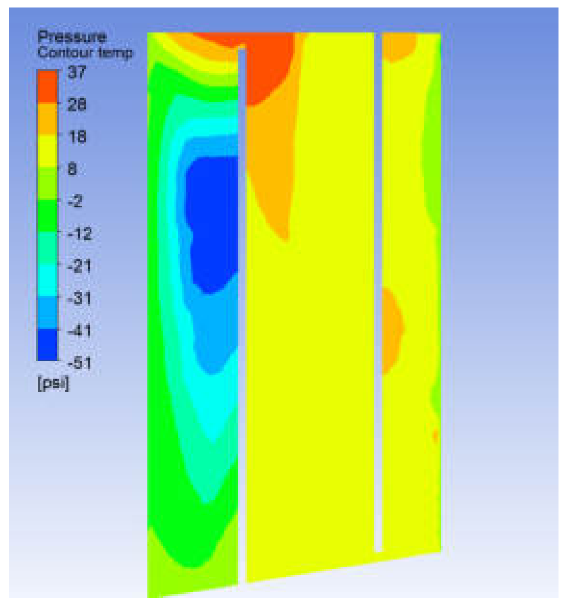

Figure 24: Pressure Contour Across the 1st Stage at Maximum Altitude

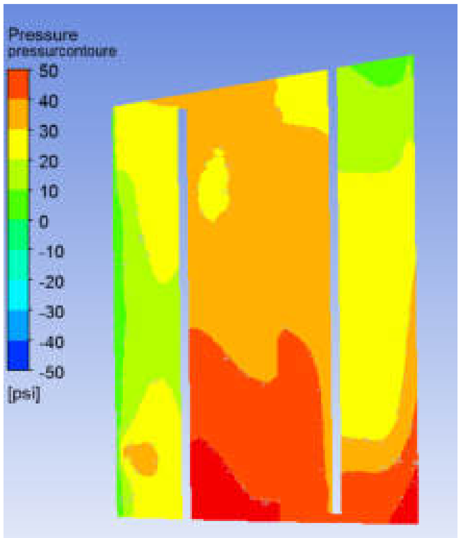

Figure 25: Pressure Contour Across the 2nd Stage at Maximum Altitude(Note image is backwards)

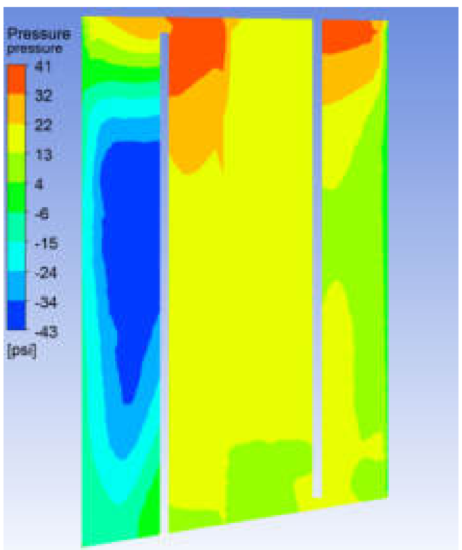

Figure 26: Pressure Contour Across the 3nd Stage at Maximum Altitude

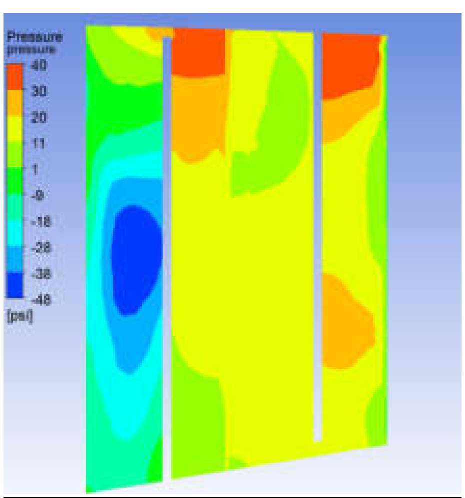

Figure 27: Pressure Contour Across the 4th Stage at Maximum Altitude

VIII. <u>Velocity Streamline plots</u>

Table 6: Area-Weighted Average Y Velocity for Compressor Stage 1

Area-Weighted Average Y Velocity	[ft/s]
Rotor Inlet	651
Rotor Outlet	651
Stator Inlet	791
Stator Outlet	848

Velocity streamline plots that demonstrate the flow patterns through the compressor stages at maximum operating altitude.

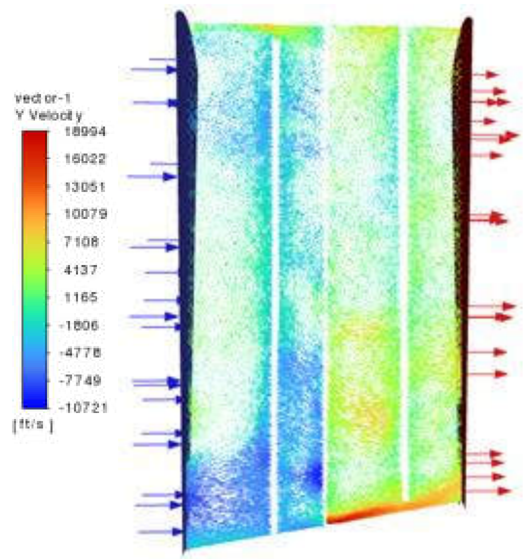

Figure 28: Velocity Streamline Plot Across Stage 1 at maximum Altitude

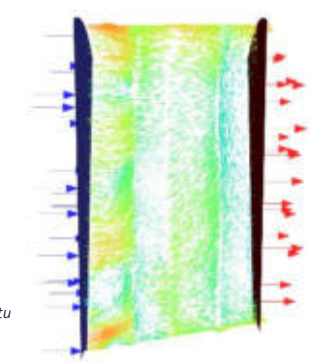

: Velocity Streamline Plot Across Stage 2 at Maximum Altitu

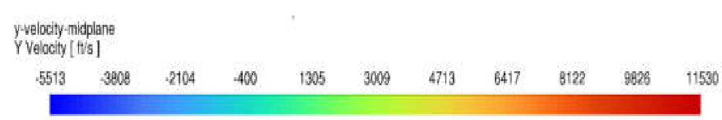

39

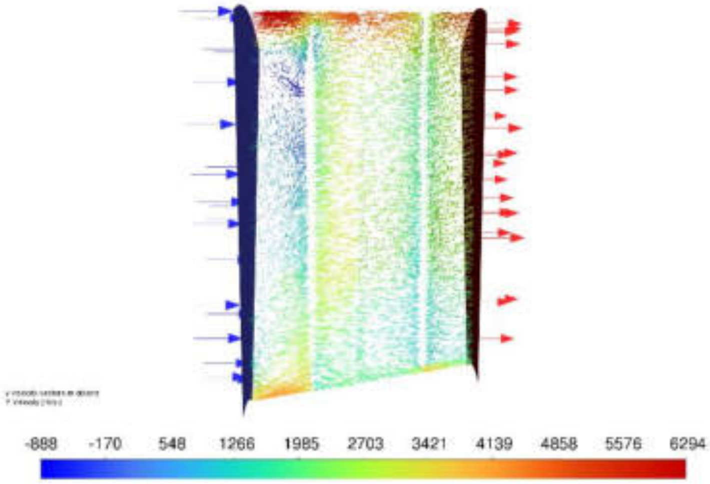

Figure 31: Velocity Streamline Plot Across Stage 3 at Maximum Altitude

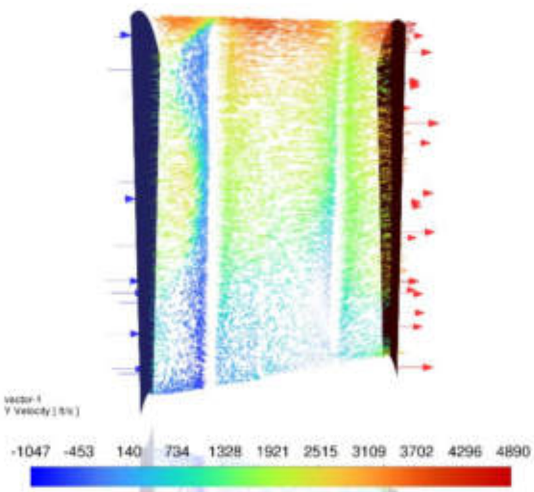

Figure 32: Velocity Streamline Plot Across Stage 4 at Maximum Altitude

IX. Summary Compression per Stage

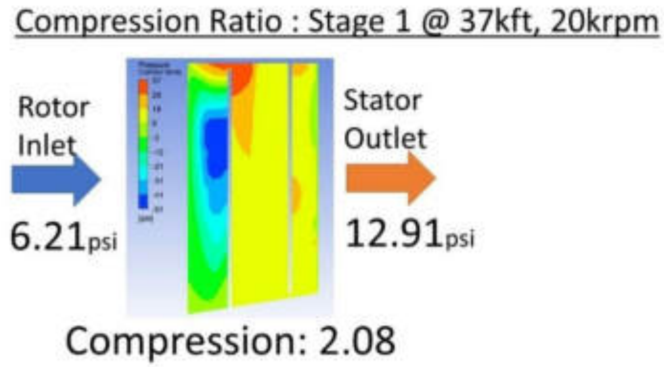

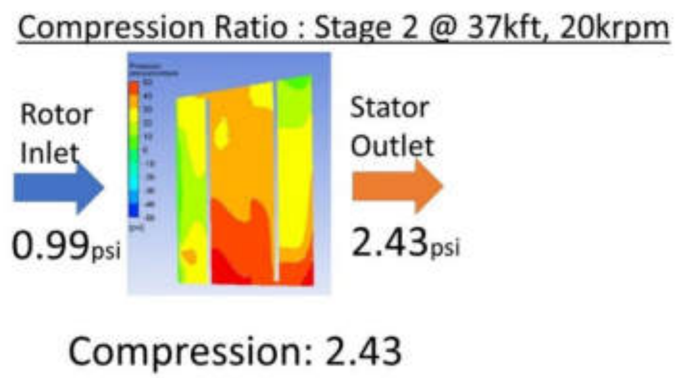

*** NB: image is flipped upside down**

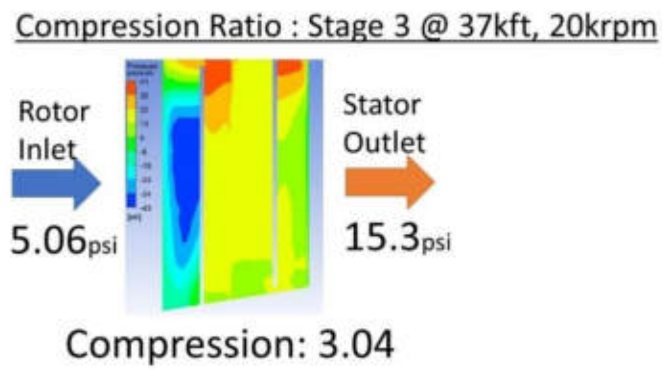

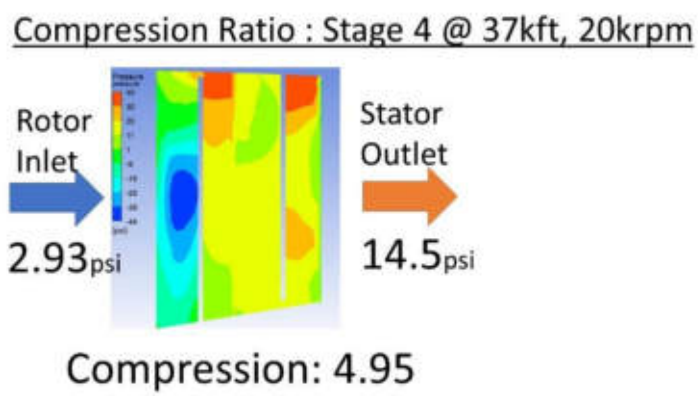

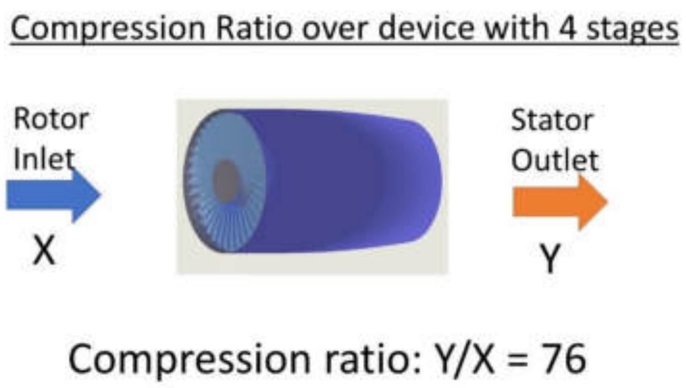

Table 7: Compression Ratio of all 4 Stages at Maximum Altitude

Stage (Pair #)	Inlet Gage (psi)	Outlet Gage (psi)	Compression Ratio
1	6.2	12.9	2.1
2	1	2.4	2.4
3	5.1	15	3.0
4	2.9	15	5.0
		Total:	76

Table 8: Compression Ratio of all 4 Stages at Maximum Altitude

Stage (Pair #)	Inlet Gage (psi)	Outlet Gage (psi)	Compression Ratio
1	0.17	12.9	5.00
2	0.12	2.4	5.62
3	(Not calculated due to goal ratio being reached)		
4			
		Total:	at least 28.1

X. Discussion

The design of a compressor is a complex problem that requires careful consideration of many factors. In this study, we approached the problem by breaking it down into slices containing a rotor and stator and using periodicity and profiles to simplify the process. We utilized Fluent and HyperMesh to perform our simulations and to develop the geometry of the compressor.

The use of periodicity and profiles allowed us to simplify the geometry of the compressor and to model it more efficiently. By designing a single slice and using periodicity to extend it to the entire compressor, we were able to reduce the computational cost of the simulation. This technique also allowed us to focus our efforts on designing an optimized slice, rather than attempting to optimize the entire compressor geometry. Furthermore, by using profiles, we were able to ensure that the flow through the compressor was smooth and efficient, while still maintaining a realistic and accurate geometry.

One disadvantage of this approach is that it requires careful consideration of the periodicity and profile designs. It can be challenging to ensure that the periodicity and profiles are optimized for the entire compressor, and small errors in these designs can result in significant differences in the simulation results. Additionally, the use of periodicity can make it difficult to accurately capture three-dimensional flow features and may not be appropriate for all types of compressors.

To simulate the flow through the compressor, we used the k-epsilon turbulence model with varying numbers of initializations and iterations. This approach allowed us to avoid floating point errors and to obtain reliable and realistic results. By varying the number of initializations and iterations, we were able to optimize the simulation settings for our specific compressor design and to ensure that our results were both accurate and efficient. The retention constants were tweaked during the process to further optimize results. The effect of retention constants on the initialization process can be significant. If the retention constants are set too low, the solver may have difficulty converging to a solution, resulting in longer simulation times and potentially inaccurate results. On the other hand, if the retention constants are set too high, the solver may converge too quickly and may not accurately capture the flow dynamics; they determine how much the solution is relaxed from the previous time step towards the new solution in the iterative process of solving the partial differential equations.

Profiles were then used to transfer information from one simulation to the other of each stage run sequentially. Using profile-based boundary conditions offers significant advantages in computational efficiency, accuracy and ease of data transfer. It ensures that there is an accurate representation of inlet conditions for each subsequent stage based on the outlet conditions of the previous stage. Modifying or updating the simulation of individual stages without the need to re-run the entire simulation was particularly valuable when design and further optimization changes were made.

XI. Conclusion

Based on simulations on what can be described as the worst-case scenarios (high altitude at full operating speed), and a start-up case at sea level, the design can be concluded to achieve the required 20:1 compression ratio.

XII. Design Time Estimate

Over the month of the project, we estimate that our team worked 360 hours for each part of the turbine design.

XIII. Appendix

a. Sample Setup conditions for Stage 1 simulations

Mesh Size

Cells	Faces	Nodes
841717	1741683	159257

Models

Model	Settings
Heat Transfer	Enabled
Space	3D
Time	Steady
Viscous	Realizable k-epsilon turbulence model
Wall Treatment	Enhanced Wall Treatment

Backflow Reference Frame	Absolute
Gauge Pressure	stator_inlet p
Pressure Profile Multiplier	1
Backflow Total Temperature	stator_inlet t0
Backflow Direction Specification Method	Direction Vector
Coordinate System	Cylindrical (Radial, Tangential, Axial)
Turbulent Specification Method	K and Epsilon
Backflow Turbulent Kinetic Energy	stator_inlet k
Backflow Turbulent Dissipation Rate	stator_inlet e
Backflow Pressure Specification	Total Pressure
Build artificial walls to prevent reverse flow?	no
Radial Equilibrium Pressure Distribution	no
Average Pressure Specification?	no
− Wall	
− rotor_4	
Wall Thickness [m]	0
Heat Generation Rate [W/m^3]	0
Material Name	aluminum
Thermal BC Type	Heat Flux
Heat Flux [W/m^2]	0
Enable shell conduction?	no
Wall Motion	Moving Wall
Shear Boundary Condition	No Slip
Define wall motion relative to adjacent cell zone?	yes
Apply a rotational velocity to this wall?	yes
Define wall velocity components?	no
Rotation Speed [rev/min]	0
X-Position of Rotation-Axis Origin [m]	0
Y-Position of Rotation-Axis Origin [m]	0
Z-Position of Rotation-Axis Origin [m]	0
Convective Augmentation Factor	1
− stator_4	
Wall Thickness [m]	0
Heat Generation Rate [W/m^3]	0
Material Name	aluminum
Thermal BC Type	Heat Flux
Heat Flux [W/m^2]	0
Enable shell conduction?	no
Wall Motion	Stationary Wall
Shear Boundary Condition	No Slip
Convective Augmentation Factor	1
− rotor_topwall	
Wall Thickness [m]	0
Heat Generation Rate [W/m^3]	0
Material Name	aluminum

Boundary Conditions

− Inlet	
− stator_inlet	
Reference Frame	Absolute
Gauge Total Pressure	rotor_outlet p0
Supersonic/Initial Gauge Pressure	rotor_outlet p
Total Temperature	rotor_outlet t0
Direction Specification Method	Direction Vector
Coordinate System	Cylindrical (Radial, Tangential, Axial)
Build artificial walls to prevent reverse flow?	no
Turbulent Specification Method	K and Epsilon
Turbulent Kinetic Energy	rotor_outlet k
Turbulent Dissipation Rate	rotor_outlet e
− rotor_inlet	
Reference Frame	Absolute
Gauge Total Pressure [psi]	0
Supersonic/Initial Gauge Pressure [psi]	0
Total Temperature [K]	300
Direction Specification Method	Direction Vector
Coordinate System	Cartesian (X, Y, Z)
Component of Flow Direction (x,y,z)	(0, 1, 0)
Build artificial walls to prevent reverse flow?	no
Turbulent Specification Method	Intensity and Viscosity Ratio
Turbulent Intensity [%]	5
Turbulent Viscosity Ratio	10
− Outlet	
− stator_outlet	
Backflow Reference Frame	Absolute
Gauge Pressure [psi]	0
Pressure Profile Multiplier	1
Backflow Total Temperature [K]	300
Backflow Direction Specification Method	Normal to Boundary
Turbulent Specification Method	Intensity and Viscosity Ratio
Backflow Turbulent Intensity [%]	5
Backflow Turbulent Viscosity Ratio	10
Backflow Pressure Specification	Total Pressure
Build artificial walls to prevent reverse flow?	no
Radial Equilibrium Pressure Distribution	no
Average Pressure Specification?	no
Specify targeted mass flow rate	no
− rotor_outlet	

Thermal BC Type	Heat Flux
Heat Flux [W/m^2]	0
Enable shell conduction?	no
Wall Motion	Stationary Wall
Shear Boundary Condition	No Slip
Convective Augmentation Factor	1
− stator_topwall	
Wall Thickness [m]	0
Heat Generation Rate [W/m^3]	0
Material Name	aluminum
Thermal BC Type	Heat Flux
Heat Flux [W/m^2]	0
Enable shell conduction?	no
Wall Motion	Stationary Wall
Shear Boundary Condition	No Slip
Convective Augmentation Factor	1
− rotor_bottom_wall	
Wall Thickness [m]	0
Heat Generation Rate [W/m^3]	0
Material Name	aluminum
Thermal BC Type	Heat Flux
Heat Flux [W/m^2]	0
Enable shell conduction?	no
Wall Motion	Moving Wall
Shear Boundary Condition	No Slip
Define wall motion relative to adjacent cell zone?	yes
Apply a rotational velocity to this wall?	yes
Define wall velocity components?	no
Rotation Speed [rev/min]	0
X-Position of Rotation-Axis Origin [m]	0
Y-Position of Rotation-Axis Origin [m]	0
Z-Position of Rotation-Axis Origin [m]	0
Convective Augmentation Factor	1
− stator_bottom_wall	
Wall Thickness [m]	0
Heat Generation Rate [W/m^3]	0
Material Name	aluminum
Thermal BC Type	Heat Flux
Heat Flux [W/m^2]	0
Enable shell conduction?	no
Wall Motion	Moving Wall
Shear Boundary Condition	No Slip
Define wall motion relative to adjacent cell zone?	yes
Apply a rotational velocity to this wall?	yes
Define wall velocity components?	no

Rotation Speed [rev/min]	0
X-Position of Rotation-Axis Origin [m]	0
Y-Position of Rotation-Axis Origin [m]	0
Z-Position of Rotation-Axis Origin [m]	0
Convective Augmentation Factor	1
− Periodic	
− stator-per	
Rotationally Periodic?	yes
− rotor-per	
Rotationally Periodic?	yes

Reference Values

Area	1 m^2
Density	1.225 kg/m^3
Enthalpy	0 J/kg
Length	1 m
Pressure	0 psi
Temperature	288.16 K
Velocity	1 m/s
Viscosity	1.7894e-05 kg/(m s)
Ratio of Specific Heats	1.4
Yplus for Heat Tran. Coef.	300
Reference Zone	rotor_fluid

Solver Settings

− Equations	
Flow	True
Turbulence	True
Energy	True
− Numerics	
Absolute Velocity Formulation	True
− Pseudo Time Explicit Relaxation Factors	
Density	1
Body Forces	1
Turbulent Kinetic Energy	0.75
Turbulent Dissipation Rate	0.75
Turbulent Viscosity	1
Energy	0.75
Explicit Momentum	0.5
Explicit Pressure	0.5
− Pressure-Velocity Coupling	
Type	Coupled
Pseudo Time Method (Global Time Step)	True

− Discretization Scheme	
Pressure	Second Order
Momentum	First Order Upwind
Turbulent Kinetic Energy	First Order Upwind
Turbulent Dissipation Rate	First Order Upwind
Energy	Second Order Upwind
− Solution Limits	
Minimum Absolute Pressure [psi]	1
Maximum Absolute Pressure [psi]	5e+10
Minimum Temperature [K]	1
Maximum Temperature [K]	5000
Minimum Turb. Kinetic Energy [m^2/s^2]	1e-14
Minimum Turb. Dissipation Rate [m^2/s^3]	1e-20
Maximum Turb. Viscosity Ratio	100000

4th stage residuals:

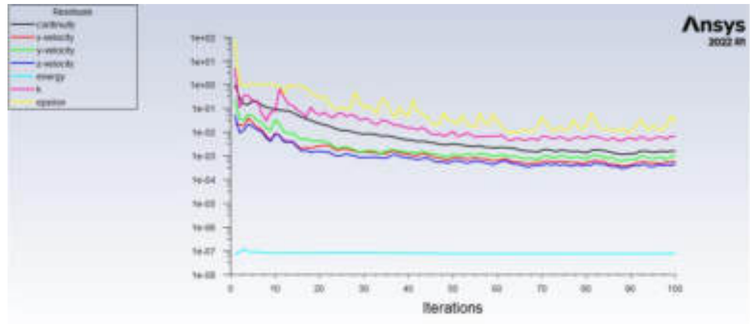

References

[1] Rojewski, Adam & Bartoszewicz, Jaroslaw. (2017). Usage of wing in ground effect to maintain lift force with reduced fuel consumption of aircraft. Combustion Engines. 169. 158-161. 10.19206/CE-2017-228.

[2] NASA. "Application of Composite Materials to Turbofan Engine Fan Exit Guide Vanes." NASA Technical Memorandum 81432, 1981..

[3] U.S. Department of Defense. "Composite Materials Handbook Volume 1: Polymer Matrix Composites Guideline for Characterization of Structural Materials." MIL-HDBK-17-1F, 2002.

[4] F. P. Incropera, D. P. DeWitt, T. L. Bergman, and A. S. Lavine, "Fundamentals of Heat and Mass Transfer", 6th ed. (Wiley, 2007).

[5] ASHRAE Handbook of Fundamentals Chapter 21

[6] Boeing 737-800: Information on the compression ratio and number of compressor stages sourced from this Boeing 737-800 brochure (https://www.boeing.com/resources/boeingdotcom/company/about_bca/startup/pdf/737_tech_specs_booklet.pdf). Compressor weight sourced from this source (https://www.prattwhitney.com/products/pw-turbofan-engines/pw-turbofan-engine-fleet/boeing-737).

[6b] Airbus A320: Information on the compression ratio and number of compressor stages sourced from this Airbus A320 brochure (https://www.airbus.com/aircraft/passenger-aircraft/a320-family.html). Compressor weight sourced from this source (https://www.prattwhitney.com/products/pw-turbofan-engines/pw-turbofan-engine-fleet/airbus-a320).

[6c] Boeing 747-8: Information on the compression ratio and number of compressor stages sourced from this Boeing 747-8 brochure (https://www.boeing.com/resources/boeingdotcom/company/about_bca/startup/pdf/747-8_tech_specs_booklet.pdf). Compressor

weight sourced from this source (https://www.geaviation.com/aircraft-engines/commercial-engines/ge90-engine/ge90-engine-specifications).

[6d] Airbus A380: Information on the compression ratio and number of compressor stages sourced from this Airbus A380 brochure (https://www.airbus.com/content/dam/corporate-topics/publications/backgrounders/tech-specs/A380_en.pdf). Compressor weight sourced from this source (https://www.rolls-royce.com/products-and-services/civil-aerospace/commercial-aircraft/airbus-a380.aspx).

[6e] Bombardier CRJ-700: Information on the compression ratio and number of compressor stages sourced from this Bombardier CRJ-700 brochure (https://commercialaircraft.bombardier.com/content/dam/Websites/bca/commercial-aircraft/support-and-services/tech-data-sheets/CRJ700-DS.pdf). Compressor weight sourced from this source (https://www.geaviation.com/aircraft-engines/regional-and-business-aviation-engines/cf34-engine/cf34-engine-specifications).

[6f] Embraer E170: Information on the compression ratio and number of compressor stages sourced from this Embraer E170 brochure (https://www.embraercommercialaviation.com/wp-content/uploads/2019/11/e170-e175_spec_sheet.pdf). Compressor weight sourced from this source (https://www.geaviation.com/aircraft-engines/regional-and-business-aviation-engines/cf34-engine/cf34-engine-specifications).

[6g] Gulfstream G650: Information on the compression ratio and number of compressor stages sourced from this Gulfstream G650 brochure (https://www.gulfstream.com/-/media/pdf/brochures/g650/g650-brochure.ashx). Compressor weight sourced from this source (https://www.rolls-royce.com/products-and-services/civil-aerospace/business-jet-engines/pearl-family.aspx).

[6h] Cessna Citation X+: Information on the compression ratio and number of compressor stages sourced from this Cessna Citation X+ brochure (https://cessna.txtav.com/-/media/files/cessna/textron-aviation/aircraft/citation-xplus/txa-xplus-spec-sheet.pdf). Compressor weight sourced from this source (https://www.txtav.com/-/media/textron-aviation/files/products/c